

Estimating the global abundance of ground level presence of microscopic particulate matter

David J. Lary¹, Fazlay Faruque², Nabin Malakar¹, Alex Moore¹, Bryan Roscoe¹, Z. Adams¹, Y. Eggelston

¹Hanson Center for Space Science, University of Texas at Dallas, Dallas, USA; ²Geographic Information Systems, University of Mississippi Medical Center, Jackson, USA

Abstract. With the increasing awareness of the health impacts of particulate matter, there is a growing need to comprehend the spatial and temporal variations of the global abundance of ground level airborne particulate matter with a diameter of 2.5 microns or less (PM_{2.5}). Here we use a suite of remote sensing and meteorological data products together with ground-based observations of particulate matter from 8,329 measurement sites in 55 countries taken 1997-2014 to train a machine-learning algorithm to estimate the daily distributions of PM_{2.5} from 1997 to the present. In this first paper of a series, we present the methodology and global average results from this period and demonstrate that the new PM_{2.5} data product can reliably represent global observations of PM_{2.5} for epidemiological studies.

Keywords: PM_{2.5}, machine-learning, remote sensing.

1 Introduction

Numerous studies show that among air pollutants, particulate matter (PM), especially with a diameter of 2.5 microns or less (PM_{2.5}), has the strongest link with human health effects (Brook et al., 2010a,b, 2013a,b; Pope et al., 2011). Increased morbidity and mortality has been associated with exposure to PM_{2.5} suggesting that improved life expectancy is possible by reducing the exposure level (Pope et al., 2009). Not only in the United States of America (USA), but also in European studies, a significant number of premature deaths, including those due to cardiopulmonary and lung cancer, are attributed to long-term exposure to PM_{2.5} (Boldo et al., 2006, 2011; Ballester et al., 2008). The many health impacts of such particulate matter (Table 1) depend in part on its abundance at ground level in the atmospheric boundary layer where it can be inhaled.

For more than half a century, researchers have been studying the impact of PM on health. Initially the attempt was to learn about the possible adverse effects; then the focus shifted to investigate the exposure-response relationships. With further advancement in technology and more awareness of health-concerns,

studies on composition-specific effects have emerged (Ayala et al., 2012). With implementation of computational fluid dynamics (CFD) models and digital imaging of organs, researchers have started to study the pathophysiology associated with PM to better understand the translocation of particulates in the human body after their deposition and how they impact health.

Most short-term exposure impact studies on PM_{2.5}, whether for morbidity or mortality, focus on cardiovascular/cardiopulmonary (Brook et al., 2010b) or respiratory (Dockery et al., 1993) conditions. Our dataset, with daily temporal scale, is suitable for such studies. We are already studying daily asthma-related hospital admissions associated with PM_{2.5} using our estimated data. On the other hand, diseases, such as lung cancer, require study of long-term exposure. Data generated from this study are expected to contribute to Health Impact Assessment (HIA) in different parts of the world concerning long-term exposure to PM_{2.5}. Currently, long-term values are not available in many localities and in many instances, PM_{2.5} values are estimated from PM₁₀ for long-term HIA (Boldo et al., 2011). Studies also suggest that even low-level PM_{2.5} exposure can contribute to serious health impacts (Pope et al., 2006; Franklin et al., 2007; Crouse et al., 2012; Cesaroni et al., 2014). We have already created daily global estimates of PM_{2.5} with an associated uncertainty for more than 13 years providing an appropriate dataset for extended cohort studies for the areas with both high and mid-level concentrations of ambient PM_{2.5}. In addition, long-range trans-

Corresponding author:

David Lary

Hanson Center for Space Science

University of Texas at Dallas, Dallas, USA

Tel. +1 972 489-2059; Fax +1 972 883-2761

E-mail: david.lary@utdallas.edu

1 Table 1. Particulate matter and health outcomes for PM₁₀, PM_{2.5} and ultrafine particles (UFPs).

Health outcomes	Short-term studies			Long-term studies		
	PM ₁₀	PM _{2.5}	UFP	PM ₁₀	PM _{2.5}	UFP
Mortality						
All causes	xxx	xxx	x	xx	xx	x
Cardiovascular	xxx	xxx	x	xx	xx	x
Pulmonary	xxx	xxx	x	xx	xx	x
Pulmonary effect						
Lung function, e.g. PEF	xxx	xxx	xx	xxx	xxx	
Lung function growth				xxx	xxx	
Asthma and COPD exacerbation						
Acute respiratory symptoms		xx	x	xxx	xxx	
Medication use			x			
Hospital admission	xx	xxx	x			
Lung cancer						
Cohort				xx	xx	x
Hospital admission				xx	xx	x
Cardiovascular effects						
Hospital admission	xxx	xxx		x	x	
ECG-related endpoints						
Autonomic nervous system	xxx	xxx	xx			
Myocardial substrate and vulnerability		xx	x			
Vascular function						
Blood pressure	xx	xxx	x			
Endothelial function	x	xx	x			
Blood markers						
Pro inflammatory mediators	xx	xx	xx			
Coagulation blood markers	xx	xx	xx			
Diabetes	x	xx	x			
Endothelial function	x	x	xx			
Reproduction						
Premature birth	x	x				
Birth weight	xx	x				
IUR/SGA	x	x				
Fetal growth						
Birth defects	x					
Infant mortality	xx	x				
Sperm quality	x	x				
Neurotoxic effects						
Central nervous system		x	xx			

2 x = few studies; xx = many studies; xxx = large number of studies.

3 portation of particles as, such dust can provide poten-
 4 tial vectors for bacteria (Ginoux and Torres, 2003;
 5 Prospero, 2003). With global coverage of this study,
 6 tracking PM_{2.5} transport is now easier for public
 7 health surveillance.

8 In recent years, researchers are finding it worthy to
 9 investigate potential links between PM_{2.5} exposure and
 10 adverse birth outcomes (Slama et al., 2008; Dadvand

11 et al., 2013), epigenetic alteration (Baccarelli et al.,
 12 2008; Salam et al., 2012; Byun et al., 2013; Hou et al.,
 13 2013) infant mortality (Woodruff et al., 1997; Lipfert
 14 et al., 2000; Dales et al., 2004; Glinianaia et al., 2004)
 15 atherosclerosis (Araujo et al., 2008; Araujo, 2011;
 16 Kaufman, 2011), stroke (Brook, 2008; Brook and
 17 Rajagopalan, 2009, 2012; Maheswaran et al., 2010,
 18 2012), rheumatic autoimmune disease (Zeft et al.,

2009; Farhat et al., 2011), central nervous system disorders (Sunderman, 2001; Kreyling et al., 2006; Block and Calderon-Garciduenas, 2009; Pearson et al., 2010; Wang et al., 2012) and diabetes (Andersen, 2012; Andersen et al., 2012). Since many of these health conditions are interlinked, comprehensive studies are required to better understand the impact of PM_{2.5}. With increasing availability of electronic health records, reliable PM_{2.5} data with seamless temporal and geographic coverage can contribute to revealing many unknowns of PM_{2.5} impacts on health.

It could be noted that the type and degree of adverse effect greatly depends on the composition of the particulate matters. Composition mostly varies due to source materials. Our current study does not provide information on the composition of PM_{2.5}. However, this study can be extended to examine the potential of source apportionment considering land use / land cover conditions and transportation mechanisms. Recent studies show specific adverse impacts of exposure to ultrafine particles (UFPs). Future studies are recommended to derive further size fractions beyond just PM_{2.5}, particularly UFPs in the sub-micron size range. Various networks of ground-based sensors routinely measure the abundance of PM_{2.5}. However, the spatial coverage has many large gaps and in some countries no observations are made at all. Globally more observations of PM₁₀ are available than for PM_{2.5}. This paper focuses on PM_{2.5}, which has been related to a wider variety of health conditions than PM₁₀ or UFPs (Table 1).

Several studies have sought to overcome this limitation of spatial coverage by using remote sensing and satellite-derived Aerosol Optical Depth (AOD) coupled with regression and/or numerical models to estimate the ground-level abundance of PM_{2.5} (e.g. Engel-Cox et al., 2004a; Zhang et al., 2009, 2011; Hoff and Christopher, 2009; Weber et al., 2010). Studies have shown that the relationship between PM_{2.5} and AOD is not always suitable for simple regression models. Rather it is determined by a multi-variate function of a large number of parameters, including: humidity, temperature, boundary layer height, surface pressure, population density, topography, wind speed, surface type, surface reflectivity, season, land use, normalised variance of rainfall events, size spectrum and phase of cloud particles, cloud cover, cloud optical depth, cloud top pressure and the proximity to particulate sources releasing PM_{2.5} (Liu et al., 2005; Lyamani et al., 2006; Choi et al., 2008; Paciorek et al., 2012; Zhang et al., 2009). The picture is further complicated by the biases present in satellite AOD products (e.g.

Lary et al., 2009; Hyer et al., 2011; Shi et al., 2012; Reid et al., 2013), the difference in spatial scales of the in-situ point PM_{2.5} observations and remote sensing data (several km per pixel) and, finally, the sharp PM_{2.5} gradients that can exist in and around cities.

Zhang et al. (2009) presented a comprehensive study for the ten Environmental Protection Agency (EPA) regions across USA using multi-linear regression between the PM_{2.5} abundance observed by the EPA monitoring sites and the Moderate Resolution Imaging Spectroradiometer (MODIS), AOD and a set of meteorological parameters. In their multi-linear regression study (Zhang et al., 2009) found the best correlations of PM_{2.5} with AOD in the eastern states during summer and autumn, with EPA region number 4 having a correlation coefficient of more than 0.6. They observed the poorest correlation for the southwestern USA, with EPA region number 9 having a correlation coefficient of approximately 0.2. Weber et al. (2010) extended the work by Zhang et al. (2009) for five EPA monitoring sites in the Baltimore/Washington DC Metro area by considering AOD from MODIS, the Multi-Angle Imaging Spectroradiometer (MISR) and the Geostationary Operational Environmental Satellite (GOES). These PM_{2.5} estimates are made available through the Infusing satellite Data into Environmental Applications (IDEA) website (<http://www.star.nesdis.noaa.gov/smcd/spb/qa/>).

In a notable study, van Donkelaar et al. (2006) took the alternative approach of using remote sensing and a global transport model to present a global estimate of the long-term average PM_{2.5} concentrations between the years 2001 and 2006 using satellite observations of AOD from MODIS to estimate $\eta = \text{PM}_{2.5}/\text{AOD}$. The three-dimensional (3D) chemical transport model used was GEOS-Chem (<http://acmg.seas.harvard.edu/geos/>), and the authors found a significant spatial agreement with their estimates; the correlation coefficient for North American PM_{2.5} measurements was 0.77 and elsewhere 0.83. PM_{2.5} estimates using this approach have since been used in a variety of health studies (van Donkelaar et al., 2010a; Anderson et al., 2012; Brauer et al., 2012; Crouse et al., 2012; Hystad et al., 2012). Meanwhile, Liu et al. estimated the ground level abundance of PM_{2.5} by using scaling factors from the GEOS-Chem, GOCART models and AOD from the MISR (Liu et al., 2004, 2005, 2007a, 2009c).

This study makes five incremental contributions:

- (i) we believe we have used the most comprehensive training dataset to date for a study that empirically relates hourly *in situ* PM_{2.5} observa-

tions to remote sensing, meteorological and other contextual, environmental data. This is important as the local context of the various $PM_{2.5}$ observations varies widely and in order to have a robust estimation of the global $PM_{2.5}$ distribution, we need representative observations in a wide range of conditions. Hourly $PM_{2.5}$ observations were acquired from 1997-present from across the world. In this study we used hourly $PM_{2.5}$ data from 8,329 measurement sites in 55 countries;

- (ii) we believe we have used the widest range of contextual variables to date (over 30 identified from the literature and presented in the last section) in our analysis of the measured multivariate, non-linear, non-parametric relationship between ground based observations of $PM_{2.5}$ and remote sensing observations, meteorological observations and associated contextual information;
- (iii) we have used the most-suitable multivariate, non-linear, non-parametric machine-learning approach currently available (briefly described in the next section) and not previously used for investigating the empirical relationship between hourly in-situ $PM_{2.5}$ observations and remote sensing, meteorological and other contextual environmental data;
- (iv) we not only estimate the $PM_{2.5}$ abundance, but also provide an uncertainty estimate; and
- (v) we cover the longest time period estimating the $PM_{2.5}$ abundance on a daily basis (from September 1, 1997 to the present).

Materials and methods

Many studies have shown that the relationship between $PM_{2.5}$ and AOD is a multi-variate function of a large number of parameters (Liu et al., 2005; Lyamani et al., 2006; Choi et al., 2008; Natunen et al., 2010; Liu and Harrison, 2011). Further, many of these relationships are non-linear, some are of unknown functional form and many have non-Gaussian distributions. Therefore, any successful description of the relationship between $PM_{2.5}$ and AOD needs to be multi-variate, non-parametric (we do not know the functional form from theory) and able to deal with non-linear behaviour and non-Gaussian distributed variables. This would suggest that a machine-learning algorithm should be used.

Machine-learning can provide a valuable regression tool for empirically estimating variables of interest, when we do not have a complete theoretical descrip-

tion of a process but do have a useful set of observations. Machine-learning encompasses a broad range of algorithms (e.g. Neural Networks, Support Vector Machines, Gaussian Processes, Decision Trees, Random Forests, etc.) that can provide multi-variate, non-linear, non-parametric regression or classification based on a training dataset. We have used all of these approaches for estimating $PM_{2.5}$ and have also developed our own proprietary ensemble approach with full error estimation (a description of which is beyond the scope of this text). The key points to highlight as relevant to this study are:

- (i) the approach includes a full independent validation. A fraction of the training data is randomly selected and held back for independent validation. These validation points are shown in red in Fig. 3;
- (ii) at every location we considered, the approach provides both an estimate of the $PM_{2.5}$ abundance as well as an error estimate;
- (iii) an ensemble of independent predictors are used at every location, and our estimate of the $PM_{2.5}$ abundance is the mean of the ensemble of estimates. A full error characterisation showed that beyond an ensemble size of 6, there was no significant error reduction. However, we used an ensemble size of 12 to be completely sure we had an ensemble that was large enough;
- (iv) the approach provides a ranking of the relative importance of each of the variables used in the regression;
- (v) the approach can handle records with missing values. However, in this study we chose to ignore records with missing values.

Datasets used in machine-learning regression

PM_{2.5} data - We used as many in-situ hourly $PM_{2.5}$ observations as possible from 8,329 sites in 55 countries from August 1, 1997 to the present (shown as red squares in Fig. 1). Fig. 2 shows the spatial and temporal coverage of this training data. Most of the observation sites were in the northern hemisphere. The high-latitude satellite data coverage is greatest in summer, so the number of in-situ $PM_{2.5}$ observations with satellite overpasses is greatest in summer as can be seen by the annual summer peaks in the Figure. Having training data from as many different physical environments as possible is critical, so a wide range of diverse conditions should be incorporated in the training data. The quality of the global machine-learning estimates of $PM_{2.5}$ improved dramatically with the inclusion of

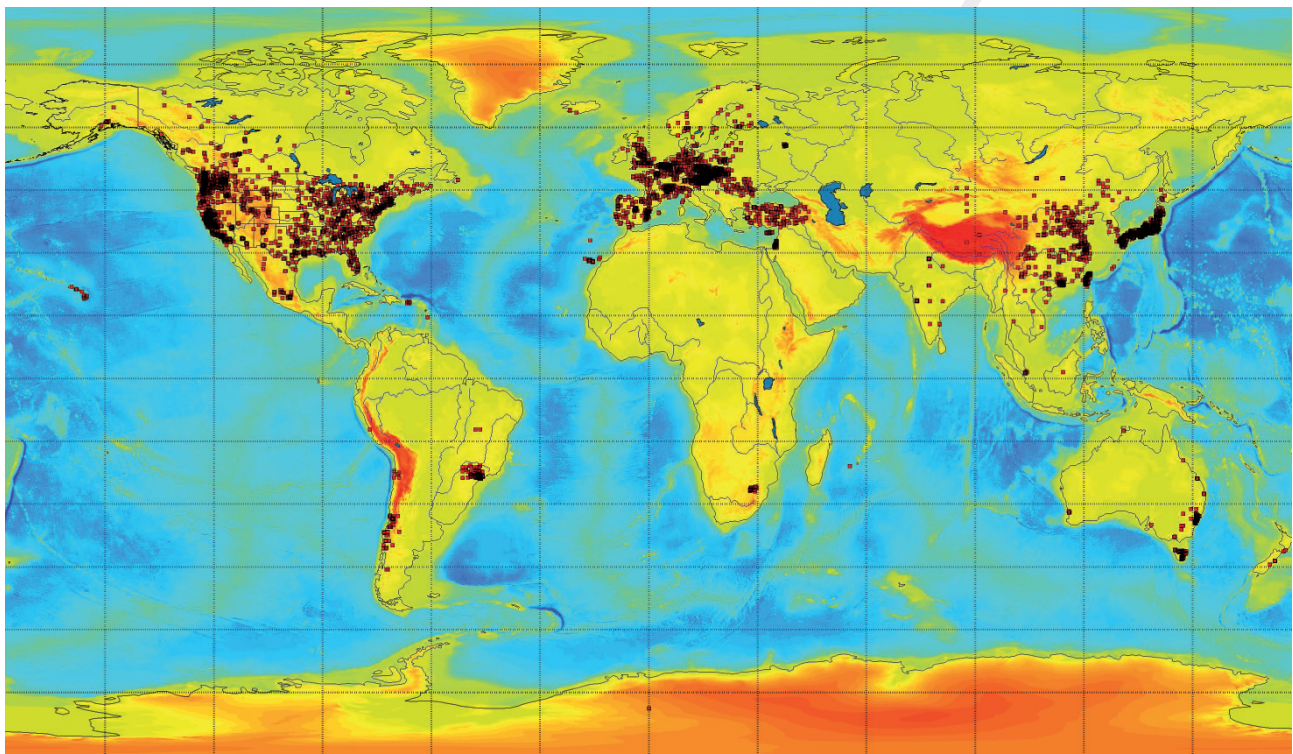


Fig. 1. Map showing the 8,329 $PM_{2.5}$ measurement site locations from 55 countries studied 1997-2014. Black squares show sites, where measurements were made against the background colour scale of global topography and bathymetry. North America, Europe and Asia have the greatest density of sites but there are also southern hemisphere sites in South America, South Africa, Australia and New Zealand.

data from the southern hemisphere (Chile, Brazil, South Africa, Australia and New Zealand) and Asia (China, India, Japan, Taiwan and Hong Kong). A random sample comprising 5% of each training dataset was held back for independent evaluation of the $PM_{2.5}$ estimate produced using machine-learning.

Satellite AOD data - This study used satellite data from three satellite instruments: the Sea-viewing Wide Field-of-view Sensor (SeaWiFS) launched on August 1, 1997 (Melin et al., 2013). Two MODIS instruments (one onboard the Terra satellite (EOS AM) launched in 1999, the other on Aqua (EOS PM) launched in 2002) (Remer et al., 2008) were chosen, both for their coverage and their near-real time data delivery. The latest distribution of MODIS data collection 5.1 was used. In this study we used the level 2 collection 5.1 data and a spatial grid with a resolution of 10×10 km (approximately $0.1^\circ \times 0.1^\circ$). MODIS collection 5 introduced the Deep Blue algorithm for retrieval of AOD over bright arid surfaces, an approach based on the idea that desert regions are darker at shorter wavelengths so the aerosol signal is clearer when using the shorter deep blue wavelengths (Hsu et al., 2004, 2006; Sayer et al., 2013).

The MODIS aerosol data files are called MOD04

for Aqua and MYD04 for Terra. In addition to the MODIS aerosol optical depth over land and ocean, the product data files include the viewing and solar illumination geometries, surface reflectance, scattering angle, angstrom exponent and various quality and cloud flags. These additional parameters turned out to be invaluable in providing an accurate multivariate, non-parametric regression to estimate the surface abundance of $PM_{2.5}$.

In MODIS collection 5.1, Deep Blue Terra data are not available after 2007. When collection 6 is released this should be remedied, there will be greater Deep Blue data coverage and higher spatial resolution. Collection 6 will include various refinements to Deep Blue, including extended coverage to vegetated and bright land surfaces, improved cloud screening and surface reflectance and aerosol microphysical models. Many of these improvements were developed during the recent application of Deep Blue to SeaWiFS data.

Meteorological data - The meteorological data used in this study come from the NASA Modern Era Retrospective analysis for Research and Applications (MERRA) (<http://gmao.gsfc.nasa.gov/merra/>) (Rienecker et al., 2011). The historic data are available from the Modeling and Assimilation Data and

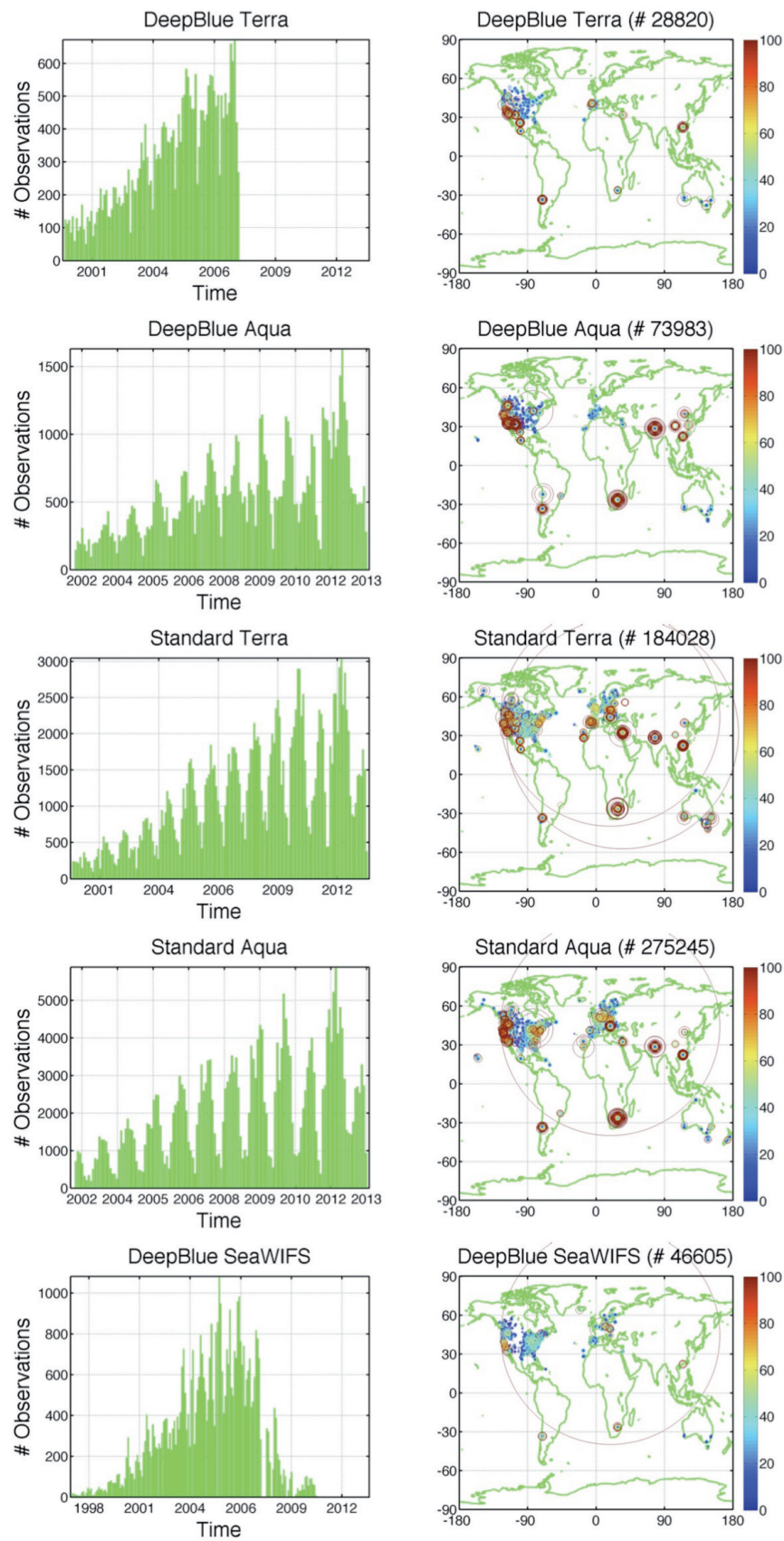


Fig. 2. Temporal (left) and spatial distribution (right) of the training data. The temporal range is different for each instrument and algorithm combination. The size of the symbols in the panels to the right is proportional to the $PM_{2.5}$ abundance.

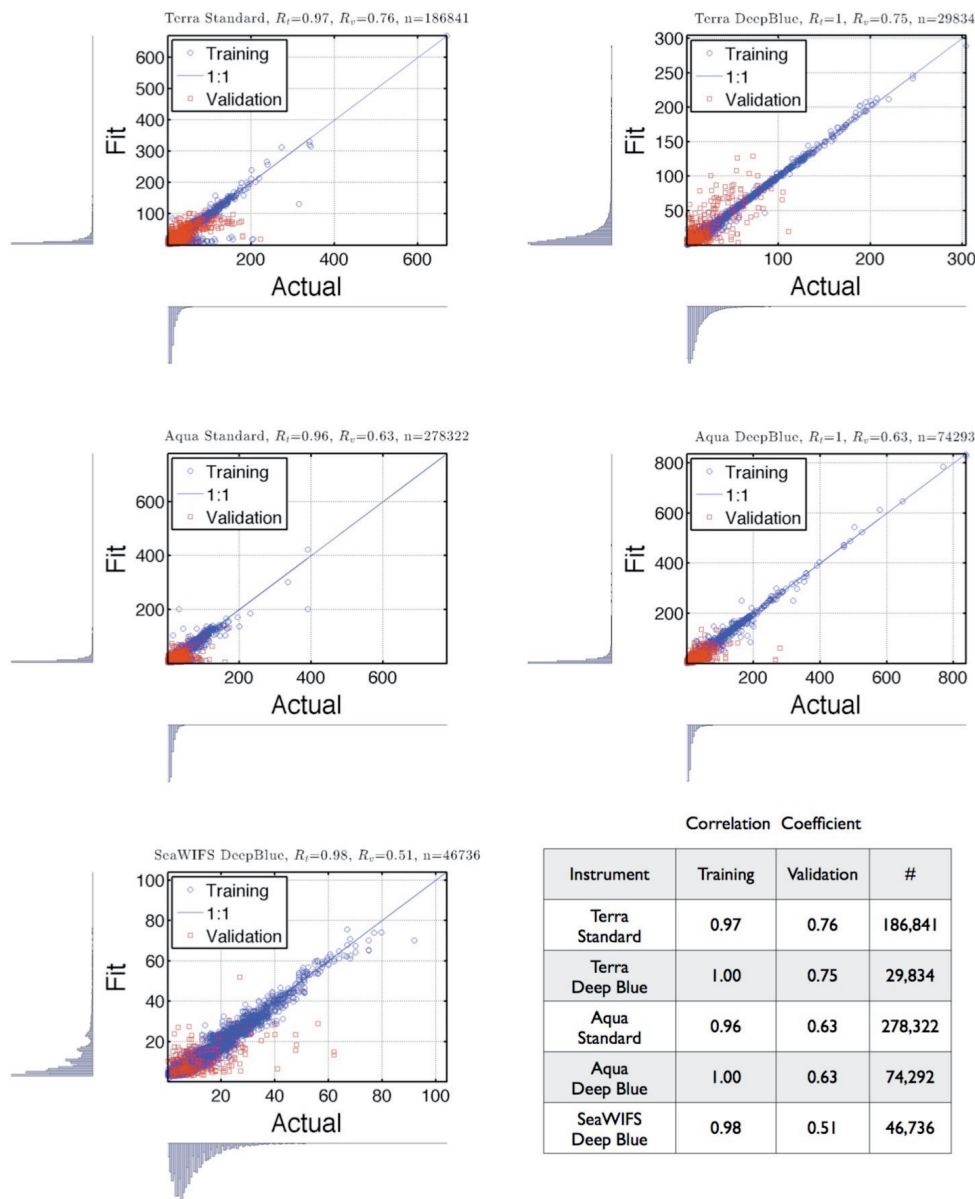
1 Information Services Center (MDISC) at
 2 <http://disc.sci.gsfc.nasa.gov/mdisc/>. The real-time and
 3 forecast data are available as part of the experimental
 4 forecast suite at <http://gmao.gsfc.nasa.gov/forecasts/>.

5
 6 *PM_{2.5} product evaluation*

7
 8 Let us now evaluate the quality of the machine-
 9 learning regression using several different approaches.

10 *Scatter diagrams* - Scatter diagrams using data for

the entire period of 1997 to present provide a visual
 means for evaluating the quality of the estimated PM_{2.5}
 abundance. A perfect fit would yield a scatter diagram
 with a slope of one and an intercept of zero. Fig. 3
 shows scatter diagrams of the observed in-situ hourly
 average PM_{2.5} abundance in $\mu\text{g}/\text{m}^3$ on the x-axis and
 the machine-learning estimate on the y-axis. The blue
 circles depict the training dataset and the red squares
 the randomly chosen independent validation dataset;
 the associated probability density function is shown



48 Fig. 3. Scatter diagrams showing the hourly average PM_{2.5} abundance. PM_{2.5} load in $\mu\text{g}/\text{m}^3$ on the x-axis and the machine-learning
 49 estimate (or fit) on the y-axis. The associated probability density function is also shown along each axis. The title of each plot shows
 50 the MODIS product used, the correlation coefficient for the training dataset (R_t), the correlation coefficient for the independent validation
 51 dataset (the 5% random selection of data left out of the training data set for independent validation - R_v, and the sample size
 52 (n)). The blue circles represent the data used in the training and the red squares the independent validation dataset. The table insert
 gives the correlation coefficients in descending order of the correlation coefficient for the independent validation dataset.

1 along each axis. The title of each panel shows the
 2 satellite data product used, the correlation coefficient
 3 for the independent training dataset R_t , the correlation
 4 coefficient for the independent validation dataset R_v ,
 5 and the sample size n . The table tabulates the correla-
 6 tion coefficients in descending order of R_v . It should be
 7 noted that the correlation coefficient for each of the
 8 five training datasets is 0.96 or greater and that the
 9 estimates (blue circles) are tightly clustered about the
 10 1:1 line. The correlation coefficient for each of the
 11 independent validation datasets (red squares) is 0.52
 12 or greater and, as would be expected, there is a little
 13 more scatter. We see that the quality varies slightly by
 14 satellite with the best fits obtained from Terra data,
 15 followed by Aqua and then SeaWIFS.

Quintile-Quintile plots - these permit comparison
 between the shapes of the observed and the estimated
 probability density functions. Two probability density
 functions of the same shape yield a straight line. For a
 good agreement we expect at least the 25th to 75th
 quintiles (the “overplotted” red squares) to form a
 straight line as it does for our machine-learning fits of
 the $PM_{2.5}$ abundance.

The probability density functions (PDF) are shown
 along each axis of the scatter diagrams in Fig. 3. We
 can see that the PDFs of the in-situ observations and
 our machine-learning estimates have very similar
 shapes. The relative shapes of the independent valida-
 tion PDFs are further tested graphically using quintile-
 quintile plots (Fig. 4). The observed $PM_{2.5}$ abundance

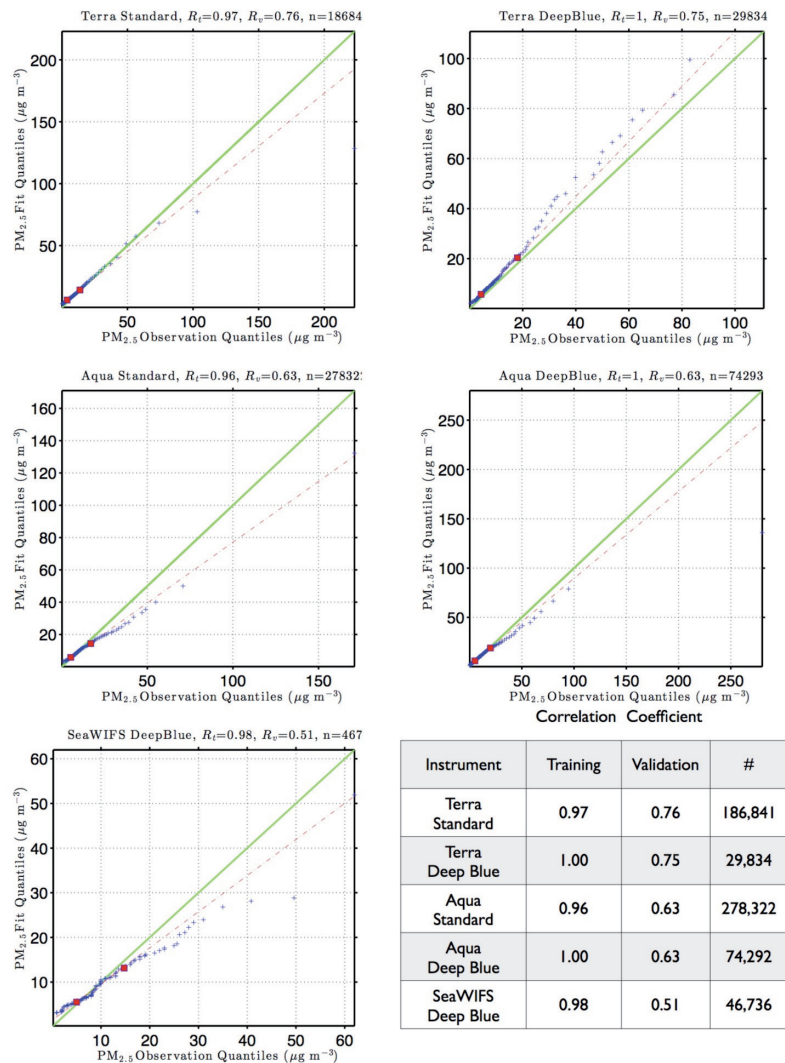


Fig. 4. Quintile-quintile diagrams for the independent validation data showing the observed quintiles of in-situ hourly average $PM_{2.5}$ abundance. $PM_{2.5}$ abundance in $\mu g/m^3$ on the x-axis and the machine-learning estimated quintiles on the y-axis. The blue circles represent the data used in the training and the red squares the independent validation dataset. The table insert gives the correlation coefficients in descending order for the independent validation dataset. Every percentile between 1 and 100 plotted.

quintiles are plotted on the x-axis and the machine-learning estimated PM_{2.5} abundance quintiles for the independent validation dataset on the y-axis. Typically the 25th to 75th quintiles of globally observed PM_{2.5} abundance falls in the range of 5-20 µg/m³. The extremely polluted areas in Asia and around some large cities are outliers (falling above the 75th quintile) in the global PM_{2.5} abundance PDF.

If the quintile-quintile plot is a straight line $y = ax + b$, but the slope is not 1. This means that the machine-learning fit and the observed data distributions differ slightly in their location and scale (Chambers et al., 1983; Fowlkes, 1987). The slope and intercept provide estimates of the scale and location. In our case the left end of the pattern is generally slightly above

the 1:1 line and the right end of the pattern is slightly below the line indicating that the PDF for the machine-learning fit has slightly shorter tails at each end of the distribution when compared to the PDF of the observations. In most cases the machine-learning approach slightly underestimates the largest PM_{2.5} abundances, but agrees with in-situ observations to within the estimated uncertainty.

Taylor diagrams - This type of graph, introduced by Taylor (2001) provides another visual way to compare the machine-learning fit to the hourly average PM_{2.5} abundance in µg/m³ to the observations (Fig. 5). The Taylor diagram quantifies the similarity between the fit and observations based on the correlation coefficient, the centred root-mean-square (RMS) difference

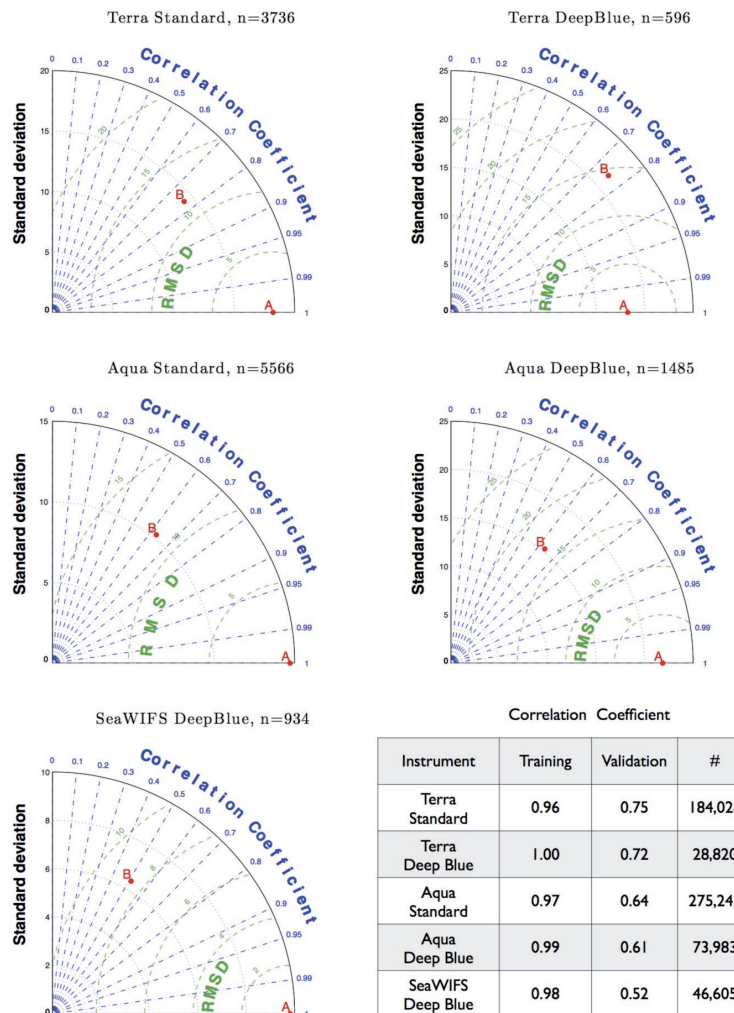


Fig. 5. Taylor diagrams quantify the similarity between the fit and observations and the amplitude of their variations, i.e. the similarity between fit and observations based on the correlation coefficient and the centred RMS difference on the one hand, and the amplitude of their variations using the standard deviation on the other. In each case, the observations are denoted by point A on the x-axis. The green contours around A show the centred RMS differences between fit and observations. The radial distance of a point from the origin is proportional to the amplitude of variation quantified by the standard deviation. Points lying on a radial arc, at the same distance from the origin as point A, have the same standard deviation indicating that the simulated variations have the correct amplitude.

1 between the fit and observations and the amplitude of
 2 their variations using the standard deviation. In each
 3 case the observations are denoted by point A on the x-
 4 axis. The green contours shown around A indicate the
 5 centred RMS differences between the fit and observa-
 6 tions. The radial distance of a point from the origin is
 7 proportional to the amplitude of variation quantified by
 8 the standard deviation. Points lying on a radial arc the
 9 same distance from the origin as point A have the same
 10 standard deviation as the observations indicating that
 11 the simulated variations have the correct amplitude. We
 12 can see from Fig. 5 that all the machine-learning fits are
 13 of reasonable quality, but those using the Deep Blue
 14 data simulate the amplitude of variation seen in the
 15 observations better than the standard algorithm.

16 *Ensemble errors* - Fig. 6 shows the ensemble training
 17 errors in $\mu\text{g}/\text{m}^3$ for our $\text{PM}_{2.5}$ abundance estimates.
 18 The blue lines show the RMS error evaluated for the
 19 training dataset and the red lines show the RMS error
 20 for the independent validation dataset. The ensemble
 21 training errors depend on how many members are in
 22 the machine-learning ensemble. There is a decrease in
 23 the error between one and six ensemble members that
 24 then plateaus with little benefit in having more than
 25 fifteen learners. In this study we have used an ensem-
 26 ble size of twelve.

28 *Multi-annual estimate of $\text{PM}_{2.5}$ abundance*

29
 30 A useful validation of the new $\text{PM}_{2.5}$ data product is
 31 to survey the key features of the global $\text{PM}_{2.5}$ distribu-
 32 tion and see if they capture, what we expect to find,
 33 and what has been reported in the literature. The
 34 upper panel of Fig. 7 shows the global average of the
 35 surface $\text{PM}_{2.5}$ abundance estimated using machine-
 36 learning of the 5,874 daily estimates from August 1
 37 1997 to August 31 2013 in $\mu\text{g}/\text{m}^3$. Overlaid as colour-
 38
 39
 40

filled circles are the observations for those locations,
 for which we have both a machine-learning estimate of
 the surface $\text{PM}_{2.5}$ abundance and an observation for
 at least one third of the 5,874 days between August 1,
 1997 to August 31, 2013. The agreement between the
 machine-learning estimate and the *in-situ* observations
 is well within the estimated uncertainty shown in the
 lower panel.

Results

Machine-learning estimates works best with a high
 volume of good quality training data (i.e. USA,
 Europe, Israel, Tasmania, a few sites in Chile and some
 parts of Asia). As can be seen in Fig. 2, the volume of
 training data has increased with time. The most signif-
 icant recent data sources have come from a network of
 Chinese monitors. Asia is probably the most challeng-
 ing region to accurately estimate $\text{PM}_{2.5}$ abundance.
 This is due to both the magnitude of the sources and
 the large spatial and temporal gradients. The estimates
 in Asia were dramatically improved by the inclusion of
 the Asian monitoring sites in our training datasets.
 The second most challenging regions are Africa and
 South America due to the paucity of observations and
 a range of large $\text{PM}_{2.5}$ sources. The inclusion of Israeli,
 South African, Mexican, Chilean and Brazilian moni-
 toring sites in our training datasets did improve the
 quality for Africa and South America. The third most
 challenging regions are Australia and New Zealand.
 The inclusion of the excellent Tasmania network as
 well as Australian and New Zealand monitoring sites
 dramatically improved the quality of our $\text{PM}_{2.5}$ abun-
 dance estimates in these countries. However, more
 $\text{PM}_{2.5}$ monitoring stations are needed in the Arabian
 peninsula, Africa, the Philippines, Indonesia, India and
 South America.

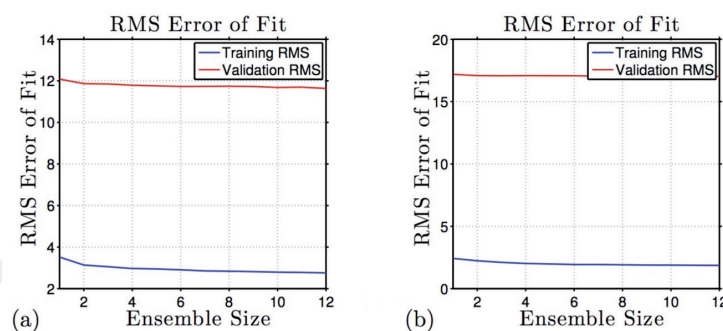


Fig. 6. Ensemble training errors in $\mu\text{g}/\text{m}^3$ for the Aqua Standard machine-learning $\text{PM}_{2.5}$ estimates (a), and the Aqua Deep Blue machine-learning $\text{PM}_{2.5}$ estimates (b). The blue lines show the RMS error evaluated for the training dataset, and the red lines the RMS error for the independent validation dataset.

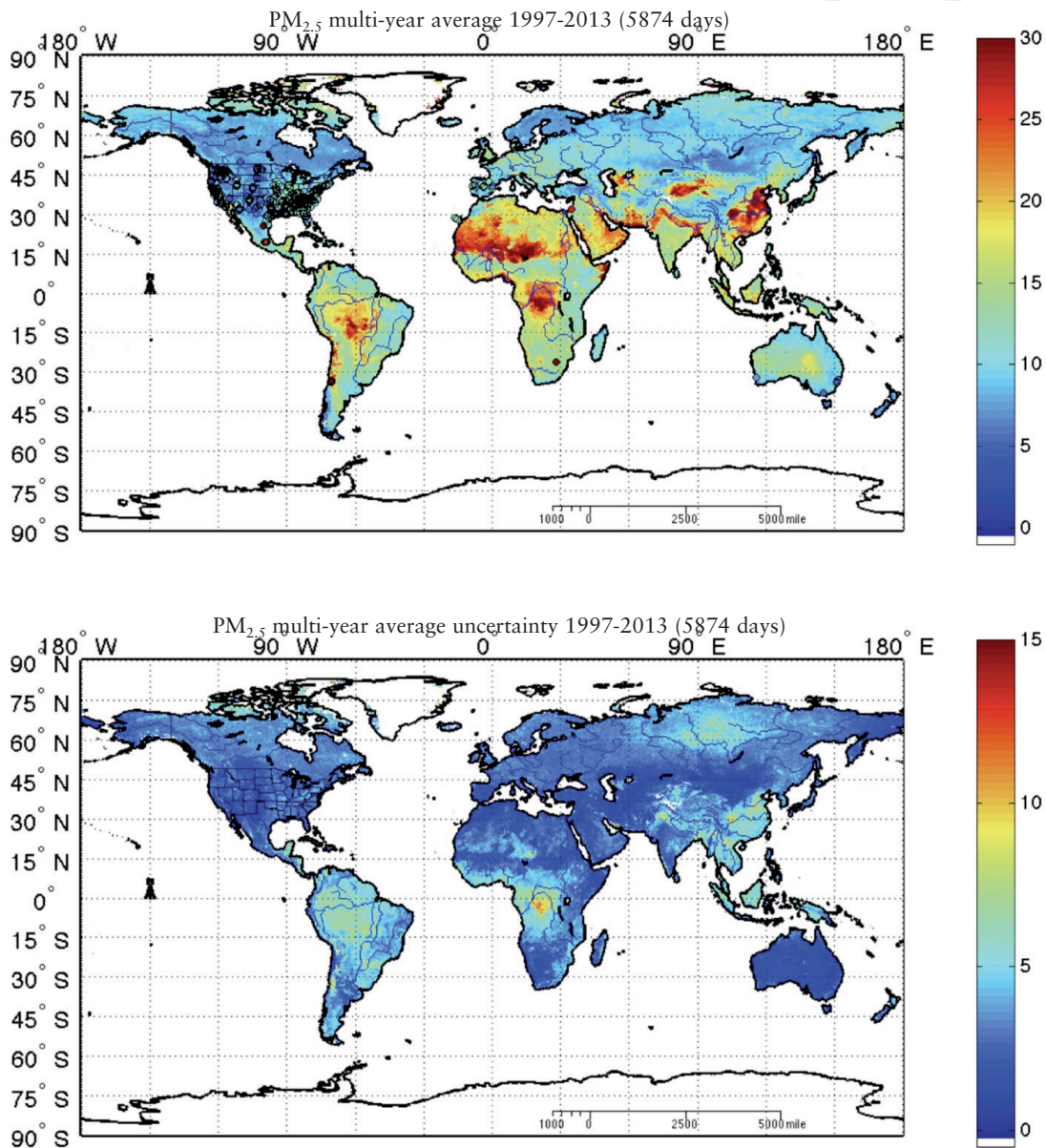


Fig. 7. The global average of the surface PM_{2.5} abundance of the 5,874 daily estimates from August 1 1997 to August 31 2013 (upper panel) with the estimated uncertainty (lower panel). The surface load of PM_{2.5} is expressed in µg/m³ with the observations for those locations, for which we have both a machine-learning estimate of the surface PM_{2.5} abundance and an observation *in situ* for at least one third of the 5,874, overlaid as colour-filled circles. The agreement between the machine-learning estimate and the *in situ* observations is well within the estimated uncertainty shown in the lower panel.

It is worth noting that the uncertainty estimate is provided by our machine-learning approach. Just as we learnt the behaviour of the PM_{2.5} abundance as a function of the 30 plus parameters obtained from satellites, meteorological analyses and population density estimates, we also learnt a second quantity, namely the uncertainty of our PM_{2.5} abundance as a function of the same 30 plus parameters. So for Saharan Africa and the Middle East, where there are few PM_{2.5} monitors (apart from in Israel), the uncertainty is based objectively on

how well the machine-learning algorithm was able to estimate the PM_{2.5} abundance for that part of the parameter space defined by the 30 plus parameters covering AOD, temperature, humidity etc. Sporadic wildfires and biomass burning are a major source of PM_{2.5} in places such as sub-Saharan Africa, Amazonia, parts of Mexico, western USA, etc. These sporadic sources are not so pronounced in Fig. 7 as it represents such a long-term average as 5,874 daily estimates from August 1 1997 to August 31 2013. However, the burning in

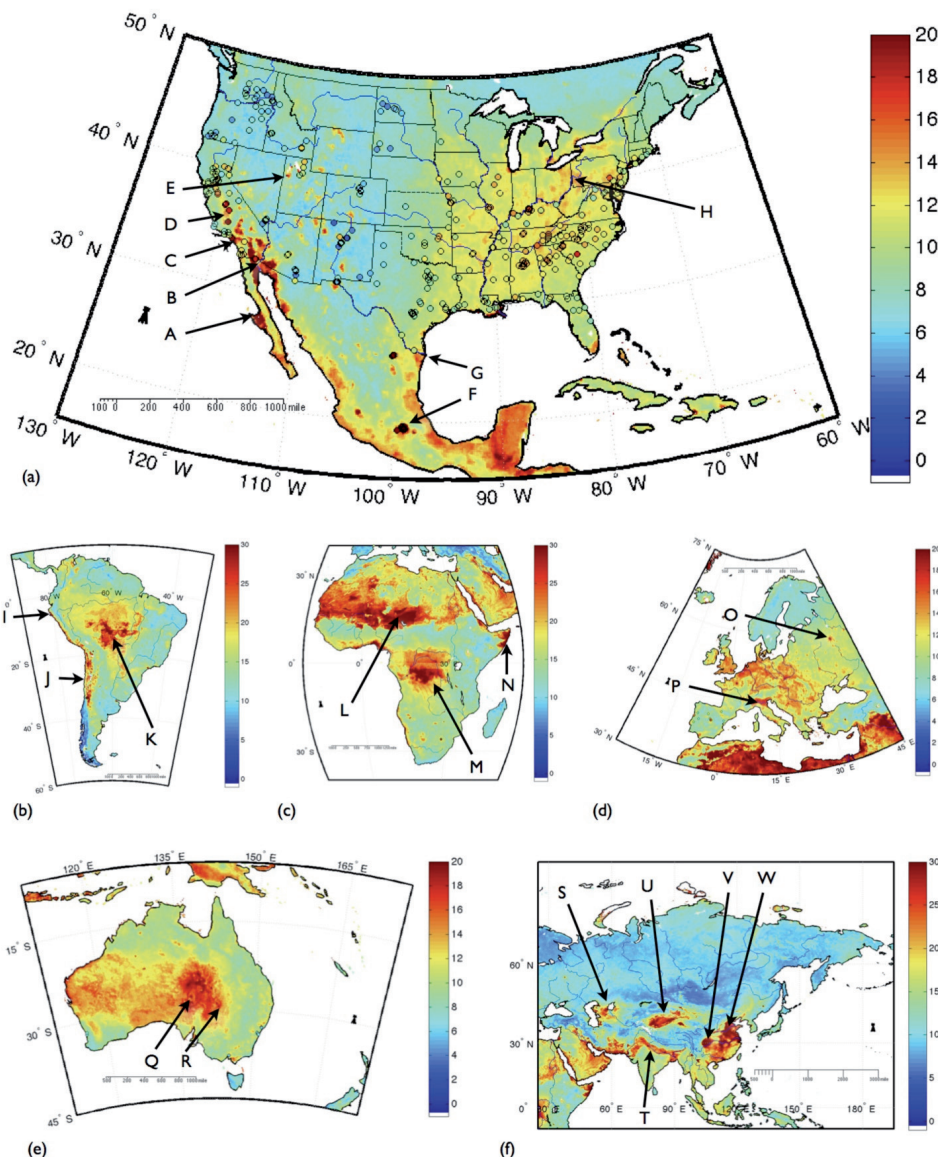
1 some regions is so persistent that it is evident even in the
 2 long-term average, e.g. in the Democratic Republic of
 3 Congo (marked M in Fig. 8).

4 Key features by region

5
 6
 7 *The Americas* - In Fig. 8a we see that the eastern half
 8 has a higher average abundance of $PM_{2.5}$ than the west-
 9 ern half of the USA with the exception of California

(Herner et al., 2005). This is consistent with the over-
 laid EPA observations shown as colour-filled circles.
 The fill for the observations uses the same colour scale
 as the machine-learning background estimates. There
 are persistently high levels of $PM_{2.5}$ in Mexico's dusty
 and desolate Baja California Sur. The particularly high
 values are in Muleg Municipality close to Guerrero
 Negro (A). The Sonoran Desert (B), a region charac-
 terised by high average $PM_{2.5}$ abundance and

12 $PM_{2.5}$ Multi-Year Average 1997-2013 (5874 days)



48 Fig. 8. The average of the surface $PM_{2.5}$ abundance of the 5,874 daily estimates from August 1, 1997 to August 31 2013 in $\mu\text{g}/\text{m}^3$
 49 for the world's inhabited continents. Particularly high levels of $PM_{2.5}$ are found in Muleg Municipality close to Guerrero Negro (A);
 50 the Sonoran Desert (B); Los Angeles (C); Central Valley in California (D); Great Salt Lake Desert, Utah (E); Mexico City (F); the
 51 Chihuahuan and the Big Bend deserts (G); Ohio River Valley (H); Piura Desert (I); coast from Andean Altiplano Basin to Neuquen
 52 Basin (J); Amazon area, Bolivia (K); Bodelle depression in Chad (L); south of Congo River (M); coastal Somalia (N); Moscow (O);
 Po Valley (P); Lake Eyre (Q); Strzelecki Desert (R); Aral Sea (S) Ganges Valley (T); Taklimakan Desert (U); Sichuan Basin (V); and
 the region from Beijing to Guangxi in China (W).

1 American dust storms (Haboobs) (Idso et al., 1972;
2 Vasquez et al., 1998; Wilt et al., 1998), straddles the
3 region close to the Mexico, Arizona and California
4 borders (Brazel and Nickling, 1978; Holcombe et al.,
5 1997). It covers an area of 311,000 km² and is one of
6 the hottest and dustiest parts of North America. This
7 is clearly evident in the high 16-year average PM_{2.5}
8 abundance in this region.

9 The persistently high PM_{2.5} abundance associated
10 with Los Angeles (C) is visible. As observed by van
11 Donkelaar et al. (2006), the regions of high popula-
12 tion density coincide with the region of high particu-
13 late abundance. California's heavily agricultural
14 Central Valley (D) has a high PM_{2.5} load (note the
15 good agreement of our estimates with the 16 year
16 average observations). The EPA has designated
17 Central Valley as a non-attainment area for the 24-
18 hour PM_{2.5} National Ambient Air Quality Standards
19 (NAAQS). The high PM_{2.5} abundance associated with
20 the Great Salt Lake Desert in northern Utah (E) close
21 to the Nevada border stands out. There is a nearby
22 measurement "supersite" at Salt Lake City (Long
23 et al., 2003) recording a particulate abundances con-
24 sistent with our estimates.

25 Mexico City is known for its high levels of particu-
26 lates and is clearly visible as a localised hotspot (F).
27 Close to the Mexico/Texas border we see the elevated
28 PM_{2.5} abundance associated with the Chihuahuan
29 Desert and the Big Bend Desert (G). Dust storms in
30 this area often impact El Paso in Texas and Ciudad
31 Juarez in Mexico (Rivera et al., 2010, 2009; Baddock
32 et al., 2011). The Ohio River Valley (H) encompasses
33 several states and is home to numerous coal-fired
34 power plants, chemical plants and industrial facilities,
35 leading to high levels of ambient particulates (Khosah
36 et al., 2000; Anderson et al., 2004; Yatavelli et al.,
37 2006; Kim et al., 2007). The Ohio River Valley has a
38 higher average abundance of PM_{2.5} than the rest of the
39 East Coast. Our analysis agrees closely with the *in-*
40 *situ* observations reported by (Yatavelli et al., 2006)
41 for the Athens "supersite". The Piura Desert in north-
42 ern Peru (I) on the coast and western slopes of the
43 Andes is a region of high particulate abundances. The
44 region in South America (J) stretching from the high
45 Andean semi-arid Altiplano basin in the North, com-
46 ing down through the Salar de Uyuni Desert (the
47 world's largest salt flats), passing by Santiago in Chile
48 (Koutrakis et al., 2005) and San Miguel de Tucumán,
49 San Juan and Mendoza in Argentina and down to the
50 Neuquen Basin in the South is characterised by a high
51 abundance of particles from a combination of dust,
52 salt and pollution. The southern Amazon in Bolivia

and the surrounding region (K) has a lot of burning
leading to persistently high particulate abundances.

Africa - The Bodelle depression (L) is Chad's lowest
point on the Sahara's southern edge that supplies the
Amazon forest with the majority of its mineral dust
(Washington and Todd, 2005; Koren et al., 2006;
Washington et al., 2006a,b; Todd et al., 2007; Bouet
et al., 2012). The high abundance of PM_{2.5} over the
Bodelle is clearly visible. Typically, there are dust
storms originating from the Bodelle depression
around 100 days a year. Washington and Todd (2005)
examined the dynamical controls of the Bodelle low-
level jet features. The major source of the world's
Aeolian dust is the Sahara (Goudie and Middleton,
2001; Middleton and Goudie, 2001). The low, flat
area that is Western Sahara is some of the most inhosp-
itable and arid land on earth and a substantial dust
source, clearly visible in the high abundance of PM_{2.5}.
Burning in the Democratic Republic of Congo (M)
leads to high levels of particulates. Much of coastal
Somalia (N) is desert characterised by high levels of
particulates.

Europe - An example of a local pollution hotspot in
Europe is Moscow (O). Otherwise, the Italian Po
Valley (P) has some of the highest average fine particle
abundance in Europe with industrial emissions cou-
pled with persistent fog leading to smog (Zappoli et
al., 1999; Schaap et al., 2002; Putaud et al., 2004;
Crosier et al., 2007).

Australia - Lake Eyre (Q) is Australia's largest lake
and lowest point, but it usually only fills with water
after heavy rains that typically occur only every three
years; otherwise it consists of a salt crust. When the
lake does fill, the depth is usually up to 1.5 m; once in
a decade it will fill up to 4 m, after which the level
falls by around 30 cm a month. When Lake Eyre has
dried out, it is Australia's largest dust source, while
the PM_{2.5} abundance there and in its vicinity is lower
than usual during the periods when it is filled with
water. Just east of the Lake Eyre Basin is the Strzelecki
Desert (R), another major Australian dust source. The
arid region just south of the Hamersley Range in
Western Australia, i.e. the Gibson Desert, Great
Victoria Desert and MacDonnell Ranges, are also
dusty environments with elevated average abundances
of PM_{2.5}.

Asia - Asia has some of the highest particulate
abundances anywhere on Earth. The Aral Sea (S)
lying across the border of Kazakhstan and
Uzbekistan is heavily polluted with major public
health problems. The Ganges Valley (T) is home to
100 million people and is highly polluted. The cold
Taklimakan Desert of northwest China (U) has an

1 area of 337,000 km² and is a major source of PM_{2.5},
2 and so is the situation in the Sichuan the Sichuan
3 Basin (V) and in the western China in the region from
4 Beijing in the North down to Guangxi in the South
5 (W).

6 Discussion

7
8
9 A PM_{2.5} data product useful for human health stud-
10 ies needs to resolve both spatial and temporal variabil-
11 ity. Figs. 3 and 4 show that our machine-learning
12 approach well reproduces the shape of the probability
13 distributions of the globally observed PM_{2.5} abun-
14 dance. Figs. 7 and 8 show that it also reproduces the
15 global average spatial distributions well.

16 A strength of this study is the daily global coverage
17 from 1997 to the present. However, as a consequence
18 of having a wide array of point sources, the PM_{2.5}
19 abundance can contain high spatial variability on
20 small scales. The spatial resolution of our study is 10
21 x 10 km (approximately 0.1° x 0.1°) determined by
22 the spatial resolution of the MODIS collection-5
23 aerosol products. Spatial variability on scales smaller
24 than 10 km is present. However, they are unresolved
25 in our data product and there are also data gaps due
26 to both cloud coverage and the difficulty that the
27 standard MODIS retrieval algorithm has with
28 retrievals over bright surfaces. MODIS collection-6 is
29 about to be released and will help address several of
30 these issues. This collection will have 3-km resolution
31 and greater Deep Blue data coverage. Collection-6
32 will include various refinements, such as extended
33 coverage to vegetated and bright land surfaces,
34 improved cloud screening, surface reflectance and
35 aerosol microphysical models. In addition, any satel-
36 lite instrument has a finite life and both MODIS satel-
37 lites (Terra and Aqua) are aging. We hope data conti-
38 nuity will be provided by the recently launched
39 Visible Infrared Imaging Radiometer Suite (VIIRS) on
40 the Suomi National Polar-orbiting Partnership weath-
41 er satellite. When data quality from VIIRS becomes
42 acceptable those data can also be used. Although to
43 our knowledge, we have used more training data
44 than any other studies of PM_{2.5} estimation, there are
45 yet certain parts of the world from where we are still
46 collecting such data. This lack of uniformity in train-
47 ing data may cause some inconsistency in data prod-
48 uct quality. However, as we make progress in acquir-
49 ing more ground PM_{2.5} data from different parts of
50 the world with missing information, the quality of
51 our dataset will be improved for those parts of the
52 world as well.

Conclusions

A new approach to use ground-based observations of PM together with a suite of remote sensing and meteorological data products training a machine-learning algorithm to estimate the daily distributions of PM_{2.5} has been demonstrated. This new PM_{2.5} daily global data product reproduces global observations and spans an unprecedented 16 years from 1997 to the present. The correlation coefficient for each of the five training datasets is 0.96 or greater and the correlation coefficient for each of the independent validation datasets is 0.52 or greater. The quality varies slightly with satellite, with the best fits obtained from Terra data, followed by Aqua and SeaWiFS. In all cases the shape of PM_{2.5} data product reproduces the observations between the 25th and 75th quantiles. The machine-learning PM_{2.5} data product is useful for human health studies as it resolves both spatial and temporal variability.

Acknowledgments

It is a pleasure to acknowledge the Institute for Integrative Health, the University of Texas at Dallas, DoD TATRC for Award W81XWH-11-2-0165, Grant Number R21ES019713 from the National Institute of Environmental Health Sciences and NASA for research funding through the award NNX11AL18G. The content is solely the responsibility of the authors and does not necessarily represent the official views of the funding agencies. It is a pleasure to acknowledge the environment agencies of Albania, Australia, Austria, Azores Islands, Belarus, Belgium, Brazil, Canada, Canary Islands, Chile, China, Croatia, Cyprus, Czech Republic, Denmark, Estonia, Finland, France, Germany, Greece, Hong Kong, Hungary, Iceland, Ireland, Israel, Italy, Japan, Latvia, Lithuania, Madeira Islands, Malaysia, Mexico, Mongolia, New Zealand, Netherlands, Norway, Peru, Poland, Portugal, Russia, Singapore, Slovakia, South Africa, South Korea, Spain, Sweden, Taiwan, Thailand, United Kingdom, United States and Vietnam for the use of their PM_{2.5} observations.

References

- Andersen ZJ, 2012. Health effects of long-term exposure to air pollution: an overview of major respiratory and cardiovascular diseases and diabetes. *Chem Ind Chem Eng Q* 18, 617-622.
- Andersen ZJ, Raaschou-Nielsen O, Ketzel M, Jensen SS, Hvidberg M, Loft S, Tjønneland A, Overvad K, Sorensen M, 2012. Diabetes incidence and long-term exposure to air pollution a cohort study. *Diabetes Care* 35, 92-98.
- Anderson HR, Butland BK, van Donkelaar A, Brauer M,

- 1 Strachan DP, Clayton T, van Dingenen R, Amann M,
2 Brunekreef B, Cohen A, et al., 2012. Satellite-based estimates
3 of ambient air pollution and global variations in childhood
4 asthma prevalence. *Environ Health Perspect* 120, 1333-1339.
- 5 Anderson RR, Martello DV, White CM, Crist KC, John K,
6 Modey WK, Eatough DJ, 2004. The regional nature of PM_{2.5}
7 episodes in the upper Ohio River Valley. *J Air Waste Manag*
8 *Assoc* 54, 971-984.
- 9 Araujo JA, 2011. Particulate air pollution, systemic oxidative
10 stress, inflammation, and atherosclerosis. *Air Qual Atmos*
11 *Health* 4, 79-93.
- 12 Araujo JA, Barajas B, Kleinman M, Wang X, Bennett BJ, Gong
13 KW, Navab M, Harkema J, Sioutas C, Lulis AJ, Nel AE, 2008.
14 Ambient particulate pollutants in the ultrafine range promote
15 early atherosclerosis and systemic oxidative stress. *Circ Res*
16 102, 589-596.
- 17 Ayala A, Brauer M, Mauderly JL, Samet JM, 2012. Air pollu-
18 tants and sources associated with health effects. *Air Qual*
19 *Atmos Health* 5, 151-167.
- 20 Baccarelli A, Barretta F, Dou C, Zhang X, McCracken JP, Diaz
21 A, Bertazzi PA, Schwartz J, Wang S, Hou L, 2011. Effects of
22 particulate air pollution on blood pressure in a highly exposed
23 population in Beijing, China: a repeated-measure study.
24 *Environ Health* 10, 108.
- 25 Baccarelli A, Tarantini L, Bonzini M, Apostoli P, Pegoraro V,
26 Bollati V, Marinelli B, Cantone L, Rizzo G, Hou L, et al.,
27 2008. Effects of particulate matter on genomic DNA methyl-
28 ation content and inos promoter methylation. *Epidemiology*
29 19, S259-S260.
- 30 Baccarelli A, Wright RO, Bollati V, Tarantini L, Litonjua AA,
31 Suh HH, Zanobetti A, Sparrow D, Vokonas PS, Schwartz J,
32 2009. Rapid DNA methylation changes after exposure to traf-
33 fic particles. *Am J Respir Crit Care Med* 179, 572-578.
- 34 Baddock MC, Gill TE, Bullard JE, Dominguez Acosta M, Rivera
35 NIR, 2011. Geomorphology of the Chihuahuan Desert based
36 on potential dust emissions. *J Maps* 2011, 249-259.
- 37 Ballester F, Medina S, Boldo E, Goodman P, Neuberger M,
38 Iniguez C, Kunzli N, Apheis N, 2008. Reducing ambient levels
39 of fine particulates could substantially improve health: a mor-
40 tality impact assessment for 26 European cities. *J Epidemiol*
41 *Community Health* 62, 98-105.
- 42 Block ML, Calderon-Garciduenas L, 2009. Air pollution: mech-
43 anisms of neuroinflammation and CNS disease. *Trends*
44 *Neurosci* 32, 506-516.
- 45 Boldo E, Linares C, Lumbreras J, Borge R, Narros A, Garcia-
46 Perez J, Fernandez-Navarro P, Perez-Gomez B, Aragones N,
47 Ramis R, et al., 2011. Health impact assessment of a reduction
48 in ambient PM_{2.5} levels in Spain. *Environ Int* 37, 342-348.
- 49 Boldo E, Medina S, LeTertre A, Hurley F, Muecke HG, Ballester
50 F, Aguilera I, Eilstein D, Apheis, G, 2006. Apheis: health
51 impact assessment of long-term exposure to PM_{2.5} in 23
52 European cities. *Eur J Epidemiol* 21, 449-458.
- Bouet C, Cautenet G, Bergametti G, Marticorena B, Todd
MC, Washington R, 2012. Sensitivity of desert dust emissions
to model horizontal grid spacing during the bodele dust exper-
iment 2005. *Atmos Environ* 50, 377-380.
- Brauer M, Amann M, Burnett RT, Cohen A, Dentener F, Ezzati
M, Henderson SB, Krzyzanowski M, Martin RV,
Van Dingenen R, et al., 2012. Exposure assessment for esti-
mation of the global burden of disease attributable to outdoor
air pollution. *Environ Sci Technol* 46, 652-660.
- Brazel AJ, Nickling WG, 1987. Dust storms and their relation to
moisture in the Sonoran-Mojave desert region of the
Southwestern United States. *J Environ Manage* 24, 279-291.
- Brook RD, 2008. Cardiovascular effects of air pollution. *Clin*
Sci (Lond) 115, 175-187.
- Brook RD, Bard RL, Kaplan MJ, Yalavarthi S, Morishita M,
Dvonch JT, Wang L, Yang H-Y, Spino C, Mukherjee B, et al.,
2013. The effect of acute exposure to coarse particulate matter
air pollution in a rural location on circulating endothelial pro-
genitor cells: results from a randomized controlled study. *Inhal*
Toxicol 25, 587-592.
- Brook RD, Rajagopalan S, 2009. Particulate matter, air pollu-
tion, and blood pressure. *J Am Soc Hypertens* 3, 332-350.
- Brook RD, Rajagopalan S, 2012. Can what you breathe trigger
a stroke within hours? *Arch Intern Med* 172, 235-236.
- Brook RD, Rajagopalan S, Pope C, Arden I, Brook JR,
Bhatnagar A, Diez-Roux AV, Holguin F, Hong Y, Luepker RV,
et al., 2010a. Particulate matter air pollution and cardiovascu-
lar disease an update to the scientific statement from the
American Heart Association. *Circulation* 121, 2331-2378.
- Brook RD, Xu X, Bard RL, Dvonch JT, Morishita M, Kaciroti
N, Sun Q, Harkema J, Rajagopalan S, 2013. Reduced meta-
bolic insulin sensitivity following sub-acute exposures to low
levels of ambient fine particulate matter air pollution. *Sci Total*
Environ 448, 66-71.
- Byun HM, Panni T, Motta V, Hou L, Nordio F, Apostoli P,
Bertazzi PA, Baccarelli AA, 2013. Effects of airborne pollu-
tants on mitochondrial dna methylation. *Part Fibre Toxicol*
10, 18.
- Cesaroni G, Forastiere F, Stafoggia M, Andersen ZJ, Badaloni
C, Beelen R, Caracciolo B, de Faire U, Erbel R, Eriksen KT, et
al., 2014. Long term exposure to ambient air pollution and
incidence of acute coronary events: prospective cohort study
and meta-analysis in 11 European cohorts from the ESCAPE
Project. *BMJ* 348, 12.
- Chambers JM, Cleveland WS, Kleiner B, Tukey PA, 1983.
Graphical methods for data analysis, Wadsworth International
Group, Belmont, Calif.
- Chen JC, Schwartz J, 2009. Neurobehavioral effects of ambient
air pollution on cognitive performance in us adults. *Neurotoxicology*
30, 231-239.
- Choi YS, Ho CH, Chen D, Noh YH, Song, CK, 2008. Spectral
analysis of weekly variation in PM₁₀ mass concentration and

- 1 meteorological conditions over China. *Atmos Environ* 42,
2 655-666.
- 3 Crosier J, Allan JD, Coe H, Bower KN, Formenti P, Williams PI,
4 2007. Chemical composition of summertime aerosol in the Po
5 Valley (Italy), Northern Adriatic and Black Sea. *Q J Roy*
6 *Meteor Soc* 133, 61-75.
- 7 Crouse DL, Peters PA, van Donkelaar A, Goldberg MS,
8 Villeneuve PJ, Brion O, Khan S, Atari DO, Jerrett M, Pope
9 C, et al., 2012. Risk of non accidental and cardiovascular mor-
10 tality in relation to long-term exposure to low concentrations
11 of fine particulate matter: A Canadian national-level cohort
12 study. *Environ Health Perspect* 120, 708-714.
- 13 Dadvand P, Parker J, Bell ML, Bonzini M, Brauer M, Darrow
14 LA, Gehring U, Glinianaia SV, Gouveia N, Ha EH, et al.,
15 2013. Maternal exposure to particulate air pollution and term
16 birth weight: A multi-country evaluation of effect and hetero-
17 geneity. *Environ Health Perspect* 121, 367-373.
- 18 Dales R, Burnett RT, Smith-Doiron M, Stieb DM, Brook JR,
19 2004. Air pollution and sudden infant death syndrome.
20 *Pediatrics* 113, E628-E631.
- 21 De Prins S, Koppen G, Jacobs G, Dons E, Van de Mierop E,
22 Nelen V, Fierens F, Panis LI, De Boever P, Cox B, et al., 2013.
23 Influence of ambient air pollution on global DNA methylation
24 in healthy adults: a seasonal follow-up. *Environ Int* 59, 418-
25 424.
- 26 Dockery DW, Pope CA, Xu XP, Spengler JD, Ware JH, Fay ME,
27 Ferris BG, Speizer FE, 1993. An association between air-pollu-
28 tion and mortality in 6 United States cities. *N Engl J Med*
29 329, 1753-1759.
- 30 Engel-Cox JA, Hoff RM, Haymet ADJ, 2004.
31 Recommendations on the use of satellite remote-sensing data
32 for urban air quality. *J Air Waste Manag Assoc* 54, 1360-
33 1371.
- 34 Engel-Cox JA, Hoff RM, Rogers R, Dimmick F, Rush AC,
35 Szykman JJ, Al-Saadi J, Chu DA, Zell ER, 2006. Integrating
36 LIDAR and satellite optical depth with ambient monitoring
37 for 3-dimensional particulate characterization. *Atmos Environ*
38 40, 8056-8067.
- 39 Engel-Cox JA, Holloman CH, Coutant BW, Hoff RM, 2004.
40 Qualitative and quantitative evaluation of MODIS satellite
41 sensor data for regional and urban scale air quality. *Atmos*
42 *Environ* 38, 2495-2509.
- 43 Engel-Cox J, Oanh NTK, van Donkelaar A, Martin RV, Zell E,
44 2013. Toward the next generation of air quality monitoring:
45 particulate matter. *Atmos Environ* 80, 584-590.
- 46 Farhat SCL, Silva CA, Orione MAM, Campos LMA, Sallum
47 AME, Braga ALF, 2011. Air pollution in autoimmune rheu-
48 matic diseases: a review. *Autoimmun Rev* 11, 14-21.
- 49 Fowlkes EB, 1987. A folio of distributions: a collection of theo-
50 retical quantile-quantile plots. New York: Marcel Dekker, 540
51 pp.
- 52 Franklin M, Zeka A, Schwartz J, 2007. Association between
PM_{2.5} and all-cause and specific-cause mortality in 27 US com-
munities. *J Expo Sci Environ Epidemiol* 17, 279-287.
- Ginoux P, Torres O, 2003. Empirical TOMS index for dust
aerosol: applications to model validation and source charac-
terization. *J Geophys Res Atmos* 108, 4534.
- Glinianaia SV, Rankin J, Bell R, Pless-Mulloli T, Howel D,
2004. Does particulate air pollution contribute to infant
death? A systematic review. *Environ Health Perspect*
112, 1365-1370.
- Goudie AS, Middleton NJ, 2001. Saharan dust storms: nature
and consequences. *Earth-Sci Rev* 56, 179-204.
- Herner JD, Aw J, Gao O, Chang DP, Kleeman MJ, 2005. Size
and composition distribution of airborne particulate matter in
northern California: I-particulate mass, carbon, and water-sol-
uble ions. *J Air Waste Manag Assoc* 55, 30-51.
- Hoff RM, Christopher SA, 2009. Remote sensing of particulate
pollution from space: have we reached the promised land? *J*
Air Waste Manag Assoc 59, 642-644.
- Hoffmann B, Moebus S, Dragano N, Stang A, Moehlenkamp S,
Schmermund A, Memmesheimer M, Broecker-Preuss M,
Mann K, Erbel R, et al., 2009. Chronic residential exposure to
particulate matter air pollution and systemic inflammatory
markers. *Environ Health Perspect* 117, 1302-1308.
- Holcombe TL, Ley T, Gillette DA, 1997. Effects of prior precip-
itation and source area characteristics on threshold wind
velocities for blowing dust episodes, Sonoran Desert 1948-78.
J Appl Meteorol 36, 1160-1175.
- Hou L, Wang S, Dou C, Zhang X, Yu Y, Zheng Y, Avula U,
Hoxha M, Diaz A, McCracken J, et al., 2012. Air pollution
exposure and telomere length in highly exposed subjects in
Beijing, China: a repeated-measure study. *Environ Int* 48, 71-
77.
- Hou L, Zhang X, Dioni L, Barretta F, Dou C, Zheng Y, Hoxha
M, Bertazzi PA, Schwartz J, Wu S, et al., 2013. Inhalable par-
ticulate matter and mitochondrial DNA copy number in high-
ly exposed individuals in Beijing, China: a repeated-measure
study. *Part Fibre Toxicol* 10.
- Hou L, Zhu ZZ, Zhang X, Nordio F, Bonzini M, Schwartz J,
Hoxha M, Dioni L, Marinelli B, Pegoraro V, et al., 2010.
Airborne particulate matter and mitochondrial damage: a
cross-sectional study. *Environ Health* 9.
- Hsu NC, Tsay SC, King MD, Herman JR, 2004. Aerosol prop-
erties over bright-reflecting source regions. *IEEE Trans Geosci*
Remote Sens 42, 557-569.
- Hsu NC, Tsay SC, King MD, Herman JR, 2006. Deep blue
retrievals of Asian aerosol properties during ACE-Asia. *IEEE*
Trans Geosci Remote Sens 44, 3180-3195.
- Hyer EJ, Reid JS, Zhang J, 2011. An over-land aerosol optical
depth data set for data assimilation by filtering, correction,
and aggregation of MODIS collection 5 optical depth
retrievals. *Atmos Meas Tech* 4, 379-408.
- Hystad P, Demers PA, Johnson KC, Brook J, van Donkelaar A,

- 1 Lamsal L, Martin R, Brauer M, 2012. Spatiotemporal air pol-
2 lution exposure assessment for a Canadian population-based
3 lung cancer case-control study. *Environ Health* 11, 22.
- 4 Hystad P, Setton E, Cervantes A, Poplawski K, Deschenes S,
5 Brauer M, van Donkelaar A, Lamsal L, Martin R, Jerrett M,
6 et al., 2011. Creating national air pollution models for popu-
7 lation exposure assessment in Canada. *Environ Health*
8 *Perspect* 119, 1123-1129.
- 9 Hystad P, Setton E, Cervantes A, Poplawski K, Deschenes S,
10 Tomlins M, Martin R, Van Donkelaar A, 2009. Feasibility of
11 a Canadian land use regression model for PM_{2.5} exposure
12 assessment. *Epidemiology* 20, S191.
- 13 Idso SB, Ingram RS, Pritchard JM, 1972. An American haboob.
14 *B Am Meteorol Soc* 53, 930-935.
- 15 Ji H, Hershey GKK, 2012. Genetic and epigenetic influence on
16 the response to environmental particulate matter. *Am J Clin*
17 *Exp Immunol* 129, 33-41.
- 18 Kaufman J, 2011. An update on the multiethnic study of athero-
19 sclerosis and air pollution. *Epidemiology* 22, S226-S227.
- 20 Khosah RP, McManus TJ, Feeley TJ, 2000. Ambient fine particu-
21 late (PM_{2.5}) monitoring research for the upper Ohio River
22 Valley project. *Abstr Pap Am Chem Soc* 219, 45-49.
- 23 Kim M, Deshpande SR, Crist KC, 2007. Source apportionment
24 of fine particulate matter (PM_{2.5}) at a rural Ohio River Valley
25 site. *Atmos Environ* 41, 9231-9243.
- 26 Koren I, Kaufman YJ, Washington R, Todd MC, Rudich Y,
27 Martins JV, Rosenfeld D, 2006. The bodele depression: a sin-
28 gle spot in the Sahara that provides most of the mineral dust
29 to the Amazon forest. *Environ Res Lett* 1, 4345-4372.
- 30 Koutrakis P, Sax SN, Sarnat JA, Coull B, Demokritou P, Oyola
31 P, Garcia J, Gramsch E, 2005. Analysis of PM₁₀, PM_{2.5}, and
32 PM_{2.5}-10 concentrations in Santiago, Chile, from 1989 to
33 2001. *J Air Waste Manag Assoc* 55, 342-351.
- 34 Kreyling WG, Semmler-Behnke M, Moller W, 2006. Ultrafine
35 particle-lung interactions: does size matter? *J Aerosol Med*
36 19, 74-83.
- 37 Kumar N, Chu AD, Foster AD, Peters T, Willis R, 2011. Satellite
38 remote sensing for developing time and space resolved esti-
39 mates of ambient particulate in Cleveland, OH. *Aerosol Sci*
40 *Technol* 45, 1090-1108.
- 41 Lary DJ, Remer LA, MacNeill D, Roscoe B, Paradise S, 2009.
42 Machine learning and bias correction of MODIS aerosol opti-
43 cal depth. *IEEE Trans Geosci Remote Sens* 6, 694-698.
- 44 Lee HJ, Liu Y, Coull BA, Schwartz J, Koutrakis P, 2011a. A
45 novel calibration approach of MODIS AOD data to predict
46 PM_{2.5} concentrations. *Atmos Chem Phys* 11, 7991-8002.
- 47 Lee HJ, Liu Y, Coull B, Schwartz, Koutrakis P, 2011b. PM_{2.5}
48 prediction modeling using MODIS AOD and its implications
49 for health effect studies. *Epidemiology* 22, S215.
- 50 Lipfert FW, Zhang J, Wyzga RE, 2000. Infant mortality and air
51 pollution: a comprehensive analysis of US data for 1990. *J Air*
52 *Waste Manag Assoc* 50, 1350-1366.
- Liu Y, Chen D, Kahn RA, He, K, 2009. Review of the applica-
tions of multiangle imaging spectroradiometer to air quality
research. *Sci China Ser D Earth Sci* 52, 132-144.
- Liu Y, Franklin M, Kahn R, Koutrakis P, 2007. Using aerosol
optical thickness to predict ground-level PM_{2.5} concentrations
in the St. Louis area: a comparison between MISR and
MODIS. *Remote Sens Environ* 107, 33-44.
- Liu Y, He K, Li S, Wang Z, Christiani DC, Koutrakis P, 2012. A
statistical model to evaluate the effectiveness of PM_{2.5} emis-
sions control during the Beijing 2008 olympic games. *Environ*
Int 44, 100-105.
- Liu YJ, Harrison RM, 2011. Properties of coarse particles in the
atmosphere of the United Kingdom. *Atmos Environ* 45, 3267-
3276.
- Liu Y, Kahn RA, Chaloulakou A, Koutrakis P, 2009. Analysis of
the impact of the forest fires in august 2007 on air quality of
Athens using multi-sensor aerosol remote sensing data, mete-
orology and surface observations. *Atmos Environ* 43, 3310-
3318.
- Liu Y, Koutrakis P, Kahn R, 2007. Estimating fine particulate
matter component concentrations and size distributions using
satellite-retrieved fractional aerosol optical depth: part 1 -
method development. *J Air Waste Manag Assoc* 57, 1351-
1359.
- Liu Y, Koutrakis P, Kahn R, Turquety S, Yantosca RM, 2007.
Estimating fine particulate matter component concentrations
and size distributions using satellite-retrieved fractional
aerosol optical depth: part 2 - a case study. *J Air Waste Manag*
Assoc 57, 1360-1369.
- Liu Y, Paciorek CJ, Koutrakis P, 2009. Estimating regional spa-
tial and temporal variability of PM_{2.5} concentrations using
satellite data, meteorology, and land use information. *Environ*
Health Perspect 117, 886-892.
- Liu Y, Paciorek C, Koutrakis P, 2008. Estimating daily pm2.5
exposure in Massachusetts with satellite aerosol remote sens-
ing data, meteorological, and land use information. *Epidemiology* 19, S116.
- Liu Y, Park RJ, Jacob DJ, Li QB, Kilaru V, Sarnat, JA, 2004.
Mapping annual mean ground-level PM_{2.5} concentrations
using multiangle imaging spectroradiometer aerosol optical
thickness over the contiguous United States. *J Geophys Res*
Atmos 109, D22206.
- Liu Y, Sarnat JA, Kilaru A, Jacob DJ, Koutrakis P, 2005.
Estimating ground-level PM_{2.5} in the Eastern United States
using satellite remote sensing. *Environ Sci Technol* 39, 3269-
3278.
- Long RW, Eatough NL, Mangelson NF, Thompson W, Fiet K,
Smith S, Smith R, Eatough DJ, Pope CA, Wilson WE, 2003.
The measurement of PM_{2.5}, including semi-volatile compo-
nents, in the EMPACT program: results from the Salt Lake
City Study. *Atmos Environ* 37, 4407-4417.
- Lyamani H, Olmo FJ, Alcantara A, Alados-Arboledas L, 2006.

- 1 Atmospheric aerosols during the 2003 heat wave in southeast-
2 ern Spain I: spectral optical depth. *Atmos Environ* 40, 6453-
3 6464.
- 4 Madrigano J, Baccarelli A, Mittleman MA, Wright RO,
5 Sparrow D, Vokonas PS, Tarantini L, Schwartz J, 2011.
6 Prolonged exposure to particulate pollution, genes associated
7 with glutathione pathways, and DNA methylation in a cohort
8 of older men. *Environ Health Perspect* 119, 977-982.
- 9 Maheswaran R, Pearson T, Smeeton NC, Beevers SD, Campbell
10 MJ, Wolfe CD, 2010. Impact of outdoor air pollution on survival
11 after stroke population-based cohort study. *Stroke* 41, 869-877.
- 12 Maheswaran R, Pearson T, Smeeton NC, Beevers SD, Campbell
13 MJ, Wolfe CD, 2012. Outdoor air pollution and incidence of
14 ischemic and hemorrhagic stroke a small-area level ecological
15 study. *Stroke* 43, 22-27.
- 16 Martin RV, 2008. Satellite remote sensing of surface air quality.
17 *Atmos Environ* 42, 7823-7843.
- 18 Melin F, Zibordi G, Carlund T, Holben BN, Stefan S, 2013.
19 Validation of SeaWiFS and MODIS Aqua/Terra aerosol prod-
20 ucts in coastal regions of European marginal seas.
21 *Oceanologia* 55, 27-51.
- 22 Middleton NJ, Goudie AS, 2001. Saharan dust: sources and tra-
23 jectories. *Trans Inst Br Geogr* 26, 165-181.
- 24 Natunen A, Arola A, Mielonen T, Huttunen J, Komppula M,
25 Lehtinen KEJ, 2010. A multi-year comparison of PM_{2.5} and
26 AOD for the Helsinki region. *Boreal Environ Res* 15, 544-552.
- 27 Paciorek CJ, Liu Y, 2009. Limitations of remotely sensed
28 aerosol as a spatial proxy for fine particulate matter. *Environ*
29 *Health Perspect* 117, 904-909.
- 30 Paciorek CJ, Liu Y, 2012. Assessment and statistical modeling of
31 the relationship between remotely sensed aerosol optical depth
32 and PM_{2.5} in the Eastern United States. *Res Rep Health Eff*
33 *Inst* 167.
- 34 Paciorek CJ, Liu Y, Moreno-Macias H, Kondragunta S, 2008.
35 Spatiotemporal associations between GOES aerosol optical
36 depth retrievals and ground-level PM_{2.5}. *Environ Sci Technol*
37 42, 5800-5806.
- 38 Patel MM, Miller RL, 2009. Rapid DNA Methylation changes
39 after exposure to traffic particles: the issue of spatio-temporal
40 factors. *Am J Respir Crit Care Med* 180, 1030-1030.
- 41 Pearson JF, Bachireddy C, Shyamprasad S, Goldfine AB,
42 Brownstein JS, 2010. Association between fine particulate
43 matter and diabetes prevalence in the US. *Diabetes Care*
44 33, 2196-2201.
- 45 Pelletier B, Santer R, Vidot J, 2007. Retrieving of particulate
46 matter from optical measurements: a semiparametric
47 approach. *J Geophys Res Atmos* 112, D06208.
- 48 Pope C, Arden I, Brook RD, Burnett RT, Dockery DW, 2011.
49 How is cardiovascular disease mortality risk affected by dura-
50 tion and intensity of fine particulate matter exposure? An inte-
51 gration of the epidemiologic evidence. *Air Qual Atmos Health*
52 4, 5-14.
- Pope C, Arden I, Burnett RT, Krewski D, Jerrett M, Shi Y, Calle
EE, Thun MJ, 2009. Cardiovascular mortality and exposure
to airborne fine particulate matter and cigarette smoke shape
of the exposure-response relationship. *Circulation* 120, 941-
948.
- Pope C, Dockery, DW, 2006. Health effects of fine particulate
air pollution: lines that connect. *J Air Waste Manag Assoc*
56, 709-742.
- Prospero JM, 2003. Global dust transport over the oceans: the
link to climate. *Geochim Cosmochim Acta* 67, A384-A384.
- Putaud JP, Raes F, Van Dingenen R, Brüggemann E, Facchini
MC, Decesari S, Fuzzi S, Gehrig R, Hüglin C, Laj P, et al.,
2004. European aerosol phenomenology-2: Chemical charac-
teristics of particulate matter at kerbside, urban, rural and
background sites in Europe. *Atmos Environ* 38, 2579-2595.
- Rajeev K, Parameswaran K, Nair SK, Meenu S, 2008.
Observational evidence for the radiative impact of Indonesian
smoke in modulating the sea surface temperature of the equa-
torial Indian Ocean. *J Geophys Res Atmos* 113, D17201.
- Reid JS, Hyer EJ, Johnson RS, Holben BN, Yokelson RJ, Zhang
J, Campbell JR, Christopher SA, Girolamo LD, Giglio L, et al.,
2013. Observing and understanding the southeast Asian
aerosol system by remote sensing: an initial review and analy-
sis for the seven southeast Asian studies (7seas) program.
Atmos Res 122, 403-468.
- Remer LA, Kleidman RG, Levy RC, Kaufman YJ, Tanre D,
Mattoo S, Martins JV, Ichoku C, Koren I, Yu H, et al., 2008.
Global aerosol climatology from the MODIS satellite sensors.
J Geophys Res Atmos 113, D14S07.
- Rienecker MM, Suarez MJ, Gelaro R, Todling R, Bacmeister J,
Liu E, Bosilovich MG, Schubert SD, Takacs L, Kim GK, et al.,
2011. Merra: nasa's modern-era retrospective analysis for
research and applications. *J Clim* 24, 3624-3648.
- Rivera NIR, Gill TE, Bleiweiss MP, Hand JL, 2010. Source char-
acteristics of hazardous Chihuahuan Desert dust outbreaks.
Atmos Environ 44, 2457-2468.
- Rivera NIR, Gill TE, Gebhart KA, Hand JL, Bleiweiss MP,
Fitzgerald RM, 2009. Wind modeling of Chihuahuan Desert
dust outbreaks. *Atmos Environ* 43, 347-354.
- Ruckerl R, Schneider A, Breitner S, Cyrus J, Peters A, 2011.
Health effects of particulate air pollution: a review of epidemi-
ological evidence. *Inhal Toxicol* 23, 555-592.
- Salam MT, Byun HM, Lurmann F, Breton CV, Wang X, Eckel
SP, Gilliland FD, 2012. Genetic and epigenetic variations in
inducible nitric oxide synthase promoter, particulate pollution,
and exhaled nitric oxide levels in children. *J Allergy Clin*
Immunol 129, 232-239.
- Salam MT, Millstein J, Li YF, Lurmann FW, Margolis HG,
Gilliland FD, 2005. Birth outcomes and prenatal exposure to
ozone, carbon monoxide, and particulate matter: results from
the children's health study. *Environ Health Perspect*

- 1 113, 1638-1644.
- 2 Sayer AM, Hsu NC, Bettenhausen C, Jeong MJ, 2013.
- 3 Validation and uncertainty estimates for MODIS collection 6
- 4 "deep blue" aerosol data. *J Geophys Res Atmos* 118, 7864-
- 5 7872.
- 6 Schaap M, Apituley A, Timmermans RMA, Koelemeijer RBA,
- 7 de Leeuw G, 2009. Exploring the relation between aerosol
- 8 optical depth and PM_{2.5} at Cabauw, the Netherlands. *Atmos*
- 9 *Chem Phys* 9, 909-925.
- 10 Schaap M, Muller K, ten Brink HM, 2002. Constructing the
- 11 European aerosol nitrate concentration field from quality
- 12 analysed data. *Atmos Environ* 36, 1323-1335.
- 13 Shi Y, Zhang J, Reid JS, Hyer EJ, Hsu NC, 2012. Critical eval-
- 14 uation of the MODIS deep blue aerosol optical depth product
- 15 for data assimilation over North Africa. *Atmos Measure Tech*
- 16 *Discuss* 5, 7815-7865.
- 17 Slama R, Darrow L, Parker J, Woodruff TJ, Strickland M,
- 18 Nieuwenhuijsen M, Glinianaia S, Hoggatt KJ, Kannan S,
- 19 Hurley F, et al., 2008. Meeting report: atmospheric pollution
- 20 and human reproduction. *Environ Health Perspect* 116, 791-
- 21 798.
- 22 Sunderman FW, 2001. Review: nasal toxicity, carcinogenicity,
- 23 and olfactory uptake of metals. *Ann Clin Lab Sci* 31, 3-24.
- 24 Tarantini L, Bonzini M, Apostoli P, Pegoraro V, Bollati V,
- 25 Marinelli B, Cantone L, Rizzo G, Hou L, Schwartz J, et al.
- 26 2009. Effects of particulate matter on genomic dna methyla-
- 27 tion content and inos promoter methylation. *Environ Health*
- 28 *Perspect* 117, 217-222.
- 29 Taylor K, 2001. Summarizing multiple aspects of model per-
- 30 formance in a single diagram. *J Geophys Res* 106, 7183-7192.
- 31 Tian D, Wang Y, Bergin M, Hu Y, Liu Y, Russell AG, 2008. Air
- 32 quality impacts from prescribed forest fires under different
- 33 management practices. *Environ Sci Technol* 42, 2767-2772.
- 34 Todd MC, Washington R, Martins JV, Dubovik O, Lizcano G,
- 35 M'Bainayel S, Engelstaedter S, 2007. Mineral dust emission
- 36 from the Bodele depression, northern Chad, during Bodex
- 37 2005. *J Geophys Res Atmos* 112, D06207.
- 38 van de Kasstele J, Koelemeijer RBA, Dekkers ALM, Schaap M,
- 39 Homan CD, Stein A, 2006. Statistical mapping of PM₁₀ con-
- 40 centrations over Western Europe using secondary information
- 41 from dispersion modeling and MODIS satellite observations.
- 42 *Stoch Environ Res Risk Assess* 21, 183-194.
- 43 van Donkelaar A, Martin RV, Brauer M, Kahn R, Levy R,
- 44 Verduzco C, Villeneuve PJ, 2010. Global estimates of ambient
- 45 fine particulate matter concentrations from satellite-based
- 46 aerosol optical depth: Development and application. *Environ*
- 47 *Health Perspect* 118, 847-855.
- 48 van Donkelaar A, Martin RV, Levy RC, da Silva AM,
- 49 Krzyzanowski M, Chubarova NE, Semutnikova E, Cohen AJ,
- 50 2011. Satellite-based estimates of ground-level fine particulate
- 51 matter during extreme events: a case study of the Moscow fires
- 52 in 2010. *Atmos Environ* 45, 6225-6232.
- van Donkelaar A, Martin RV, Park RJ, 2006. Estimating
- ground-level PM_{2.5} using aerosol optical depth determined
- from satellite remote sensing. *J Geophys Res* 111, D21201.
- van Donkelaar A, Martin R, Verduzco C, Brauer M, Kahn R,
- Levy R, Villeneuve P, 2010. A hybrid approach for predicting
- PM_{2.5} exposure response. *Environ Health Perspect* 118, A425.
- Vasquez HR, Fausett J, Sipple S, Estle WT, Haro JA, Wojcik W,
- Berkovitz R, Sturm D, Cushmeer N, Jamison A, et al., 1998.
- A South-Central Arizona Haboob - the 28 July 1994 wind and
- dust storm. Part 1: event forecastability, 16th conference on
- weather analysis and forecasting / symposium on the research
- foci of the U.S. Weather Research Program.
- Villeneuve PJ, Goldberg MS, Burnett RT, van Donkelaar A,
- Chen H, Martin RV, 2011. Associations between cigarette
- smoking, obesity, sociodemographic characteristics and
- remote-sensing-derived estimates of ambient PM_{2.5}: Results
- from a Canadian population-based survey. *Occup Environ*
- Med* 68, 920-927.
- Wang BL, Li XL, Xu XB, Sun YG, Zhang Q, 2012. Prevalence
- of and risk factors for subjective symptoms in urban preschool
- children without a cause identified by the guardian. *Arch*
- Environ Occup Health* 85, 483-491.
- Wang Q, Shao M, Liu Y, William K, Paul G, Li X, Liu Y, Lu S,
2007. Impact of biomass burning on urban air quality estimat-
- ed by organic tracers: Guangzhou and Beijing as cases. *Atmos*
- Environ* 41, 8380-8390.
- Washington R, Todd MC, 2005. Atmospheric controls on min-
- eral dust emission from the Bodele depression, Chad: The role
- of the low level jet. *Geophys Res Lett* 32, L17701.
- Washington R, Todd MC, Engelstaedter S, Mbainayel S,
- Mitchell F, 2006. Dust and the low-level circulation over the
- Bodele depression, Chad: Observations from Bodex 2005. *J*
- Geophys Res Atmos* 111, D06207.
- Washington R, Todd MC, Lizcano G, Tegen I, Flamant C, Koren
- I, Ginoux P, Engelstaedter S, Bristow CS, Zender CS, et al.,
2006. Links between topography, wind, deflation, lakes and
- dust: the case of the Bodele depression, Chad. *Geophys Res*
- Lett* 33, L09401.
- Weber SA, Engel-Cox JA, Hoff RM, Prados AI, Zhang H, 2010.
- An improved method for estimating surface fine particle con-
- centrations using seasonally adjusted satellite aerosol optical
- depth. *J Air Waste Manag Assoc* 60, 574-585.
- Wilt RE, Breckenridge CA, Davis JT, Franjevic MW, Wojcik W,
- Cushmeer N, Amer Meteorol SOC, 1998. A South-Central
- Arizona Haboob - the 28 July 1994 wind and dust storm. Part
- 2: radar and satellite observations, 16th conference on weather
- analysis and forecasting / symposium on the research foci of
- the U.S. Weather Research Program.
- Woodruff TJ, Grillo J, Schoendorf KC, 1997. The relationship
- between selected causes of postneonatal infant mortality and
- particulate air pollution in the United States. *Environ Health*
- Perspect* 105, 608-612.

- 1 Woodruff TJ, Morello-Frosch R, Jesdale B, 2008. Air pollution
2 and preeclampsia among pregnant women in California,
3 1996-2004. *Epidemiology* 19, S310-S310.
- 4 Woodruff TJ, Parker JD, Schoendorf, KC, 2006. Fine particu-
5 late matter (PM_{2.5}) air pollution and selected causes of post-
6 neonatal infant mortality in California. *Environ Health*
7 *Perspect* 114, 786-790.
- 8 Yatavelli RLN, Fahrni JK, Kim M, Crist KC, Vickers CD,
9 Winter SE, Connell DP, 2006. Mercury, PM_{2.5} and gaseous co-
10 pollutants in the Ohio River Valley Region: Preliminary results
11 from the Athens supersite. *Atmos Environ* 40, 6650-6665.
- 12 Zappoli S, Andracchio A, Fuzzi S, Facchini MC, Gelencser A,
13 Kiss G, Krivacsy Z, Molnar A, Meszaros E, Hansson HC, et
14 al., 1999. Inorganic, organic and macromolecular components
15 of fine aerosol in different areas of Europe in relation to their
16 water solubility. *Atmos Environ* 33, 2733-2743.
- 17
18
19
20
21
22
23
24
25
26
27
28
29
30
31
32
33
34
35
36
37
38
39
40
41
42
43
44
45
46
47
48
49
50
51
52
- Zeft AS, Prahalad S, Lefevre S, Clifford B, McNally B, Bohnsack
JF, Pope CAI, 2009. Juvenile idiopathic arthritis and exposure
to fine particulate air pollution. *Clin Exp Rheumatol* 27, 877-
884.
- Zhang H, Hoff RM, Engel-Cox JA, 2009. The relation between
moderate resolution imaging spectroradiometer (MODIS)
aerosol optical depth and PM_{2.5} over the United States: a geo-
graphical comparison by US Environmental Protection Agency
Regions. *J Air Waste Manag Assoc* 59, 1358-1369.
- Zhang H, Lyapustin A, Wang Y, Kondragunta S, Laszlo I, Ciren
P, Hoff RM, 2011. A multi-angle aerosol optical depth
retrieval algorithm for geostationary satellite data over the
United States. *Atmos Chem Phys* 11, 11977-11991.
- Zhang J, Reid JS, 2009. An analysis of clear sky and contextual
biases using an operational over ocean MODIS aerosol prod-
uct. *Geophys Res Lett* 36.